

Guided subwavelength plasmonic mode supported by a slot in a thin metal film

Georgios Veronis and Shanhui Fan

Department of Electrical Engineering, Stanford University, Stanford, California 94305

Received July 1, 2005; revised manuscript received August 12, 2005; accepted August 23, 2005

We demonstrate the existence of a bound optical mode supported by a slot in a thin metallic film deposited on a substrate, with slot dimensions much smaller than the wavelength. The modal size is almost completely dominated by the near field of the slot. Consequently, the size is very small compared with the wavelength, even when the dispersion relation of the mode approaches the light line of the surrounding media. In addition, the group velocity of this mode is close to the speed of light in the substrate, and its propagation length is tens of micrometers at the optical communication wavelength. © 2005 Optical Society of America
OCIS codes: 130.2790, 240.6680, 260.2110.

Waveguide structures that support highly confined optical modes are important for achieving compact integrated photonic devices.^{1,2} In particular, plasmonic waveguides have shown the potential to guide subwavelength optical modes. Several different plasmonic waveguiding structures have been proposed.^{1,3–12} However, these structures support a highly confined mode only near the surface plasmon frequency. In this regime, the optical mode typically has low group velocity and a short propagation length.

In this Letter we investigate the characteristics of the bound optical mode supported by an air slot in a thin metallic film deposited on a substrate [inset of Fig. 1(a)]. This structure is hereafter referred to as a plasmonic slotline. Of particular interest is the regime where the dimensions of the slot are much smaller than the wavelength. We show that such a structure supports a fundamental bound mode with size almost completely dominated by the near field of the slot over a wide range of frequencies. The size of this mode can be far smaller than the wavelength even when its effective index approaches that of the substrate. In addition, the group velocity of the mode is close to the speed of light in the substrate and its propagation length is tens of micrometers at the optical communication wavelength. Thus, such a waveguide could be potentially important in providing an interface between conventional optics and subwavelength electronic and optoelectronic devices.

We calculate the eigenmodes of the plasmonic slotline at a given wavelength λ_0 using a full-vectorial finite-difference frequency-domain (FDFD) mode solver. For waveguiding structures that are uniform in the z direction, if an $\exp(-\gamma z)$ dependence is assumed for all field components, Maxwell's equations reduce to two coupled equations for the transverse magnetic field components H_x and H_y .¹³ These equations are discretized on a nonuniform orthogonal grid, resulting in a sparse matrix eigenvalue problem of the form $\mathbf{A}\mathbf{h} = \gamma^2\mathbf{h}$, which is solved using iterative sparse eigenvalue techniques.¹⁴ To calculate the bound eigenmodes of the waveguide, we ensure that the size of the computational domain is large enough

that the fields are negligibly small at its boundaries,¹⁵ while for leaky modes we use perfectly matched layer absorbing boundary conditions.¹⁴ An important feature of this formulation is the absence of spurious modes.¹⁵ In addition, the frequency-domain mode solver allows us to directly use experimental data for the frequency-dependent dielectric constant of metals,¹⁶ including both the real and the imaginary parts, with no further approximation. Here we define the propagation length L_p and the ef-

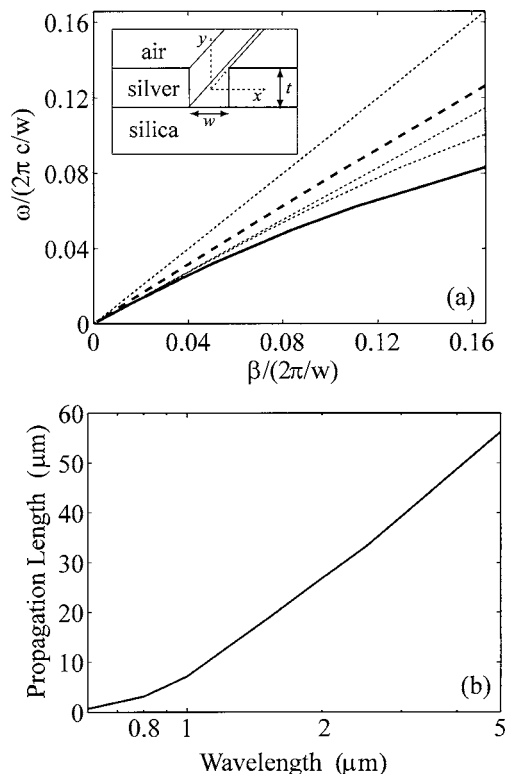


Fig. 1. (a) Dispersion relation of the fundamental mode of the plasmonic slotline (solid curve) for $w, t = 50$ nm (see inset) and of a PEC slotline (dashed curve). The upper, middle, and lower thin dotted curves are the light lines of air and silica and the lowest frequency mode of the silver film, respectively. (b) Propagation length of the fundamental mode of the plasmonic slotline as a function of wavelength for $w, t = 50$ nm.

fective index n_{eff} of a propagating mode through the equation $\gamma = L_p^{-1} + i\beta = L_p^{-1} + i2\pi n_{\text{eff}}\lambda_0^{-1}$.

In Fig. 1(a) we show the dispersion relation of the fundamental mode of the plasmonic slotline. The width w and thickness t of the slot are 50 nm, and the substrate material is silica ($n_s = 1.44$). We observe that such a structure supports a bound mode in a wide frequency range. Within this range this mode has a wave vector larger than all radiation modes in air and silica, as well as all propagating modes in the air–silver–silica thin film structure. The cutoff frequency of this mode is $\sim 0.005(2\pi c/w)$, where c is the speed of light in free space. We also found that, if the slot dimensions are smaller than 100 nm, the optical communication frequency ($\lambda_0 = 1.55 \mu\text{m}$) is well above ω_{cutoff} . Since the slot dimensions are much smaller than the wavelength in the frequency range of interest, the fundamental bound mode is quasi-TEM with dominant field components E_x and H_y , and this waveguide does not support any higher-order bound modes. Since the fundamental mode is quasi-TEM, it can be efficiently excited by linearly polarized light.

As a comparison, in Fig. 1(a) we also show the dispersion relation when the perfect electric conductor (PEC) approximation is used for the metallic regions. We observe that the PEC slotline structure on the substrate does not support a bound mode at any frequency. When the slot dimensions are far smaller than the wavelength, the fields are essentially the same as those of the static case.¹⁷ In the PEC case, the fields do not penetrate into the metal. The field lines are either in air or in silica. The effective index of the mode n_{eff} therefore satisfies the relation $1 < n_{\text{eff}} < n_s$.¹⁷ The PEC model is commonly used to describe slotlines at microwave frequencies. While such structures do not support any bound mode, in practice they guide waves effectively,^{17,18} since radiation loss turns out to be negligible for deep subwavelength structures. In comparison, the existence of a bound mode for the plasmonic slotline is entirely due to the finite negative dielectric constant of metals at optical frequencies, which results in higher n_{eff} for the fundamental mode.

In Fig. 1(b) we show the propagation length L_p of the fundamental mode of the plasmonic slotline as a function of wavelength. The propagation length decreases as the wavelength decreases. This is due to the fact that the propagation length of surface plasmons scales with the wavelength,¹⁹ since the fraction of the modal power in the metal increases at shorter wavelengths,⁶ and also due to increased material losses of metals at shorter wavelengths.¹⁶ At the optical communication wavelength of $1.55 \mu\text{m}$ the propagation length is $\sim 20 \mu\text{m}$.

In Fig. 2(a) we show the power density profile of the fundamental mode of the plasmonic slotline for $\lambda_0 = 1.55 \mu\text{m}$. We observe that the mode is confined mostly in the slot region and slightly extends to the adjacent silica and air regions. The maximum intensity is observed at the silver–air interfaces in the slot. This is expected since the mode can be seen as being formed by the coupling of the surface plasmon–

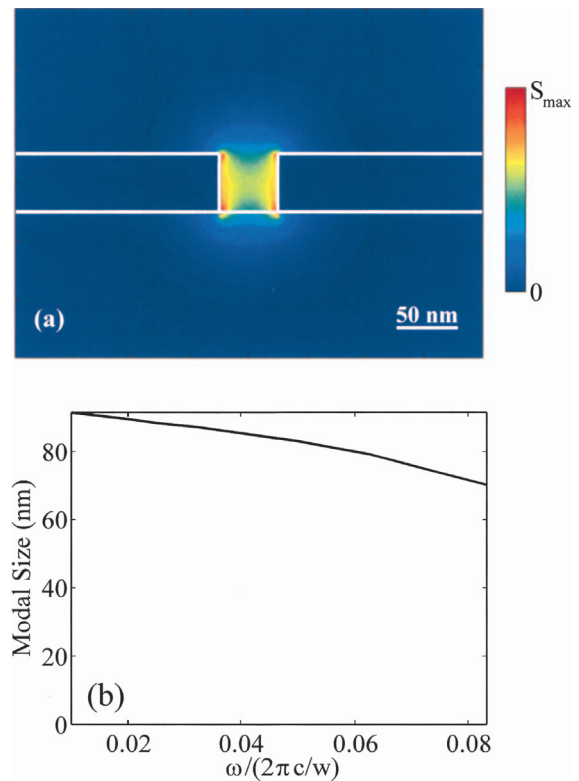


Fig. 2. (a) Power density profile at $\lambda_0 = 1.55 \mu\text{m}$, and (b) Modal size as a function of frequency of the fundamental mode of the plasmonic slotline for $w, t = 50 \text{ nm}$.

polaritons at the two silver–air interfaces. In Fig. 2(b) we show the modal size, defined as the square root of the area in which the mode power density is larger than $1/e^2$ of its maximum value, as a function of frequency. At the optical communication wavelength of $1.55 \mu\text{m}$ the modal size is $\sim 87 \text{ nm}$, which is much smaller than the minimum achievable modal sizes with high-index-contrast dielectric waveguides. For comparison, the minimum achievable modal size with square silicon waveguides embedded in silica at $\lambda_0 = 1.55 \mu\text{m}$ is $\sim 400 \text{ nm}$.²⁰ We also note that the modal size varies only weakly as a function of frequency.

We observe that the modal size remains small even at low frequencies where the dispersion relation approaches the silica light line. This behavior is fundamentally different from that of conventional dielectric waveguides. In conventional dielectric waveguides, the fields in the low-index cladding surrounding the high-index core decay exponentially with a decay constant $\alpha = 2\pi/\lambda_0 \sqrt{n_{\text{eff}}^2 - n_{\text{clad}}^2}$, where n_{clad} is the refractive index of the cladding region.²¹ In these structures, the minimum confinement of a guided optical mode is $\sim \lambda_0/(2n_{\text{core}})$, where n_{core} is the refractive index of the core region.⁴ If the dimensions of the core are reduced far below $\lambda_0/(2n_{\text{core}})$, the dispersion relation of the optical mode approaches the cladding light line ($n_{\text{eff}} \rightarrow n_{\text{clad}}$), the decay constant α becomes extremely small, and the modal size becomes extremely large.^{20,21} In contrast, in the case of the plasmonic slotline, even though the same exponential behavior should still hold in the far field, the modal size is dominated by the near field of the slot.

In Fig. 3(a) we show the power density profile of the fundamental mode of the plasmonic slotline in a vertical cut at $x=0$ [Fig. 1(a)] for $w, t = 25, 50, 100$ nm and $\lambda_0 = 1.55$ μm . This profile has two distinctive characteristics related to the near and far fields. Far from the slot, the modal power density decays asymptotically as $\sim \exp(-2\alpha\rho)/\rho$, where $\alpha = \text{Re}[-\gamma^2 - (2\pi n_{\text{clad}}/\lambda_0)^2]^{1/2}$, as expected from Maxwell's equations. If the slot dimensions w, t increase, the effective index of the mode n_{eff} decreases, and therefore the decay rate α decreases. Note also that, since $n_s = 1.44 > 1$, the decay rate is always larger in air.

In Fig. 3(b) we show the power density profile in the vicinity of the slot. We observe that the near field of the slot scales with the slot dimensions w, t and is independent of w/λ_0 . This is due to the fact that the slot dimensions are much smaller than the wavelength. In addition, silver satisfies the condition $|\epsilon_{\text{metal}}| \gg \epsilon_{\text{air}}$ at $\lambda_0 \sim 1.55$ μm .¹⁶ Thus, based on the boundary condition for the normal component of the electric field E_x at the silver–air interfaces in the slot, we have $|E_x|_{\text{metal}} \ll |E_x|_{\text{air}}$. The modal profile is there-

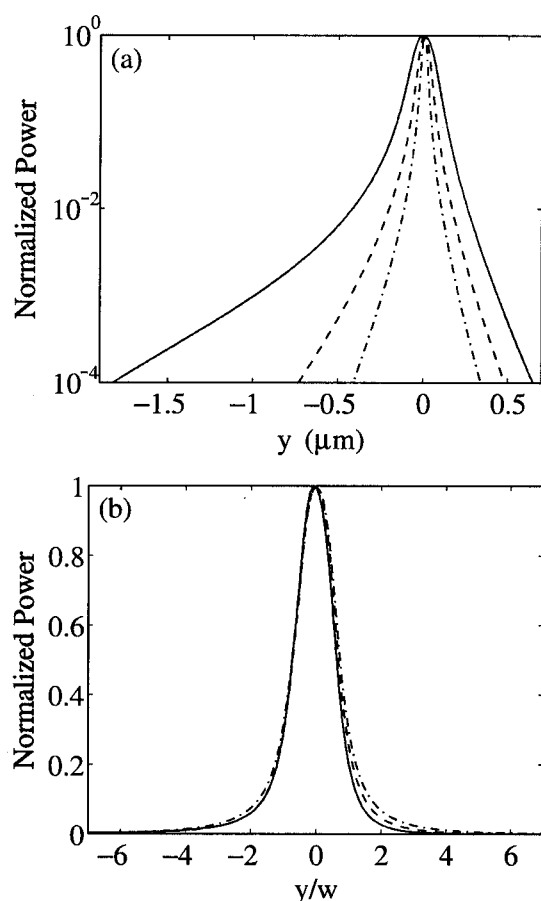


Fig. 3. (a) Power density profile at $\lambda_0 = 1.55$ μm of the fundamental mode of the plasmonic slotline at $x=0$ [Fig. 1(a)] for $w, t = 25, 50,$ and 100 nm (dashed–dotted, dashed, and solid curves, respectively). (b) Power density profile at $x=0$ in the vicinity of the slot for $w, t = 25, 50, 100$ nm. Note that the horizontal axis is normalized with respect to w .

fore highly confined in the slot region [Fig. 2(a)], and the modal size is dominated by the near field of the slot. Thus, even when the dispersion relation of the mode approaches the silica light line and the far-field decay rate α decreases, the modal size remains relatively small [Fig. 2(b)]. In addition, since the near field scales with the slot dimensions, the modal size of the plasmonic slotline can be further reduced, if the slot dimensions are reduced. We note that this comes at the cost of reduced propagation length.²²

The authors acknowledge useful discussions with D. A. B. Miller. This research was supported by DARPA/MARCO under the Interconnect Focus Center and by U.S. Air Force Office of Scientific Research grant FA 9550-04-1-0437. S. Fan's e-mail address is shanhui@stanford.edu.

References

1. J. Takahara, S. Yamagishi, H. Taki, A. Morimoto, and T. Kobayashi, *Opt. Lett.* **22**, 475 (1997).
2. V. R. Almeida, Q. Xu, C. A. Barrios, and M. Lipson, *Opt. Lett.* **29**, 1209 (2004).
3. J. J. Burke, G. I. Stegeman, and T. Tamir, *Phys. Rev. B* **33**, 5186 (1986).
4. J. C. Weeber, A. Dereux, C. Girard, J. R. Krenn, and J. P. Goudonnet, *Phys. Rev. B* **60**, 9061 (1999).
5. J. R. Krenn, B. Lamprecht, H. Ditlbacher, G. Schider, M. Salerno, A. Leitner, and F. R. Aussenegg, *Europhys. Lett.* **60**, 663 (2002).
6. P. Berini, *Phys. Rev. B* **61**, 10484 (2000).
7. M. L. Brongersma, J. W. Hartman, and H. A. Atwater, *Phys. Rev. B* **62**, R16356 (2000).
8. S. A. Maier, P. G. Kik, H. A. Atwater, S. Meltzer, E. Harel, B. E. Koel, and A. A. G. Requicha, *Nat. Mater.* **2**, 229 (2003).
9. F. Kusunoki, T. Yotsuya, J. Takahara, and T. Kobayashi, *Appl. Phys. Lett.* **86**, 211101 (2005).
10. K. Tanaka and M. Tanaka, *Appl. Phys. Lett.* **82**, 1158 (2003).
11. I. V. Novikov and A. A. Maradudin, *Phys. Rev. B* **66**, 035403 (2002).
12. D. F. P. Pile and D. K. Gramotnev, *Opt. Lett.* **29**, 1069 (2004).
13. J. A. Pereda, A. Vegas, and A. Prieto, *Microwave Opt. Technol. Lett.* **38**, 331 (2003).
14. J. Jin, *The Finite Element Method in Electromagnetics* (Wiley, 2002).
15. S. J. Al-Bader, *IEEE J. Quantum Electron.* **40**, 325 (2004).
16. E. D. Palik, ed., *Handbook of Optical Constants of Solids* (Academic, 1985).
17. D. M. Pozar, *Microwave Engineering* (Wiley, 1998).
18. E. A. Mariani, C. P. Heinzman, J. P. Agrios, and S. B. Cohn, *IEEE Trans. Microwave Theory Tech.* **17**, 1091 (1969).
19. W. L. Barnes, A. Dereux, and T. W. Ebbesen, *Nature* **424**, 824 (2003).
20. L. Vivien, S. Laval, E. Cassan, X. Le Roux, and D. Pascal, *J. Lightwave Technol.* **21**, 2429 (2003).
21. S. L. Chuang, *Physics of Optoelectronic Devices* (Wiley, 1995).
22. Similar behavior was observed in two-dimensional metal–dielectric–metal waveguide structures by R. Zia, M. D. Selker, P. B. Catrysse, and M. L. Brongersma, *J. Opt. Soc. Am. A* **21**, 2442 (2004).